

## Protein adhesion regulated by the nanoscale surface conformation†

Cite this: DOI: 10.1039/c2sm27204k

Eun Chul Cho,<sup>a</sup> Hyunjoon Kong,<sup>\*b</sup> Tae Byeong Oh<sup>c</sup> and Kilwon Cho<sup>\*c</sup>

Protein adhesion and adsorption behaviors vary in response to variations in surface wettability; however, few reports have examined the dependence of such behaviors on variations in the surface molecular conformations. This study examines the degree to which molecular disorder at the surface of a surface-modified hydrocarbon chain monolayer regulates protein adhesion. Octadecyltrichlorosilane (OTS) molecules were deposited onto silicon wafers at two temperatures, 5 °C or 55 °C, to prepare two OTS surfaces with different degrees of molecular disorder. Atomic force microscopy (AFM) was used to evaluate the nanoscale adhesion force between proteins and the two types of OTS monolayers during a short contact time (<1 s). Bovine serum albumin (BSA) and human fibrinogen (HF) adhered more strongly to the disordered than to the ordered OTS monolayer. The adhesion strength at longer contact times (30 s–90 min) was evaluated by investigating the resistance of proteins on the OTS monolayer to detachment by washing. The magnitude of the resistance could be predicted from the topologies of the monolayers, as determined by AFM, after the adsorption of proteins and the subsequent washing experiments. After a 90 min adsorption period, BSA displayed a higher resistance to detachment from the disordered OTS monolayer than from the ordered OTS monolayer. HF displayed a higher resistance to detachment from the disordered OTS monolayer for only very short adsorption times of less than 1 min. The results suggest that the proteins altered their adhesion onto monolayers with different OTS conformations and that different adsorption times were required for each protein to present the different degrees of adhesion.

Received 18th July 2012  
Accepted 22nd October 2012

DOI: 10.1039/c2sm27204k

www.rsc.org/softmatter

### 1 Introduction

Protein adsorption plays a critical role in a variety of biological processes, including cell adhesion to an extracellular matrix, the immune response to implants, and bacterial fouling of filtration membranes. The quantities and conformations of proteins adsorbed onto substrates depend strongly on the chemical and physical properties of the substrate surfaces.<sup>1–15</sup> For example, increasing the hydrophobicity of a surface significantly increases the amount of proteins adsorbed onto the surface. The conformations of proteins adsorbed onto solid substrates can depend on the chemical and physical properties of the substrates. For example, protein structures may become

denatured, or their mode of adsorption (end-on or side-on) can be altered.<sup>16,17</sup>

Significant efforts have been made toward engineering the chemical and physical properties of solid substrates for the purpose of controlling protein adsorption. Short hydrocarbon molecules and polymers with various functional groups have been chemically linked to solid substrates.<sup>1–12</sup> The densities of these surface-modifying molecules and their spatial distribution on the nano- and micrometer scale have been successfully modulated.<sup>12–15</sup> Engineered surfaces can be used to regulate the amount and type of adsorption, or they can be used to prevent adsorption.<sup>13–15</sup> Such surfaces are widely used in a variety of biomedical applications, including tissue engineering, biofouling, and biosensors.<sup>18</sup>

Protein adsorption can be regulated by varying the densities of hydrocarbon chains that have been adsorbed onto silicon substrates.<sup>13–15</sup> Choi *et al.* prepared two monolayers with different densities of hydrocarbon chains by varying the deposition time, and the monolayer density could be used to regulate the protein conformation.<sup>13b</sup> However, the use of an organic monolayer's molecular conformation to regulate protein adhesion behavior is less understood. Our previous results demonstrated that hydrocarbon monolayers can display varying degrees of adhesion to silicon nitride AFM tips depending on

<sup>a</sup>Department of Chemical Engineering, Division of Chemical and Bioengineering, Hanyang University, Seoul, 133-791, Korea

<sup>b</sup>Department of Chemical and Biomolecular Engineering, Institute for Genomic Biology, University of Illinois, Urbana Champaign, Urbana, IL 61801, USA. E-mail: hjkong06@illinois.edu

<sup>c</sup>Department of Chemical Engineering, Polymer Research Institute, Pohang University of Science and Technology, Pohang, 790-784, Korea. E-mail: kwcho@postech.ac.kr

† Electronic supplementary information (ESI) available: Procedure to estimate the adhesion energy between the proteins immobilized on the AFM tip and the substrates. See DOI: 10.1039/c2sm27204k

the monolayer conformation.<sup>19</sup> In light of these results, the degree of molecular ordering is expected to significantly modulate the effects of other substrate properties on protein adhesion.

This study examined whether the degree of disorder of surface-modifying molecules could be used to regulate protein adhesion. Silicon substrates presenting organosilane chains were prepared at two temperatures to produce organosilane monolayers with two different conformations, that is, with two degrees of intermolecular ordering. The degree of intermolecular ordering was analyzed by reflection–absorption Fourier transform infrared spectroscopy (RA-FTIR). The adhesion of two proteins, BSA and HF, onto the surface-modified substrates was investigated by measuring adhesion strength using atomic force microscopy (AFM). In addition, the adhesion was also evaluated by observing the topologies of the monolayers using the AFM after protein adsorption followed by a washing step. The structures of the solid substrates and the adhesion behaviors of the proteins were found to be correlated.

## 2 Experimental methods

### 2.1 Preparation of the organic monolayers

All organic contaminants on the silicon wafers (P-type Si(100), Shinetsu) were eliminated by immersion in piranha solution ( $\text{H}_2\text{SO}_4 : \text{H}_2\text{O}_2 = 70 : 30$ ) at 80 °C for 30 min. After rinsing with deionized water, the wafers were vacuum-dried for 3 h. Two pre-cleaned and vacuum-dried reaction flasks were charged with argon gas, and then filled with 10 mM of an octadecyltrichlorosilane (OTS, Aldrich)–toluene solution. Each flask containing the OTS–toluene solution was respectively equilibrated either at 5 °C or 50 °C. The pre-cleaned silicon wafers were then immersed into the flasks containing the OTS–toluene solution equilibrated at one of the two temperatures. The reaction between the silicon wafer and OTS was carried out for 2 h under an Ar flow. After the reaction, the silicon wafers were washed twice with toluene and once with ethanol, and then baked in a convection oven at 120 °C for 20 min. After baking, the substrates were sonicated in toluene, and then washed again with toluene and ethanol. The chemical coupling of the OTS monolayers to the silicon wafers was confirmed by RA-FTIR spectroscopy (Bruker IFS 66v FT-IR). The wettabilities of the OTS monolayers were determined by measuring the water contact angle. Ellipsometry (M-2000V, J.A. Woollam Co., Inc.) was used to determine the thickness of each OTS monolayer.

### 2.2 Measurements of the adhesion force between the OTS monolayers and the proteins

The adhesion force between the OTS monolayers and the protein molecules was measured by AFM (AutoProbe® CR Research, Park Scientific Instruments). The protein molecules were immobilized on the AFM tip surfaces as follows. First, silicon nitride AFM tips ( $\text{Si}_3\text{N}_4$ , radius of 50 nm) were exposed to oxygen plasma for one minute to generate hydroxyl groups on the tip surfaces. The AFM tips were then immediately immersed in to a 10 mM  $\gamma$ -aminopropyltriethoxysilane (Aldrich)–toluene

solution at room temperature for 2 h in order to modify the tip surfaces with amine groups. The amine-terminated AFM tips were subsequently exposed to a 10% v/v glutaraldehyde (Aldrich) aqueous solution at room temperature for 30 min. Finally, for the protein modification step, bovine serum albumin (BSA,  $M_w$  67 kDa, A8022 Sigma) or human fibrinogen (HF,  $M_w$  340 kDa, F-4883 Sigma) was each dissolved to a concentration of 1 mg mL<sup>-1</sup> in a 10 mM phosphate buffer saline (PBS) aqueous solution (pH 7.4, Aldrich). The tips were dipped into the protein solutions for 40 min. After washing with an aqueous PBS solution, the protein-modified tips were stored in PBS at 28 °C.

The AFM tips presenting immobilized proteins were used to measure the adhesion force between the proteins and the OTS monolayer. The monolayer substrate was attached to the bottom of a liquid cell, and the cell was filled with PBS solution. Then the cell was placed on the AFM stage and moved upward to immerse the AFM tip. The cell was slowly brought into close proximity to the AFM tip. At the appropriate separation distance, an interaction force could be measured between the tip and the substrate by approaching and retracting the monolayer substrates. All experiments were carried out in an aqueous PBS (10 mM, pH 7.4) solution at 28 °C. The substrate was advanced toward the tip until contact was achieved, after which the substrate was retracted. The approach and retraction distances were approximately the same, 1  $\mu\text{m}$ , covered with a velocity of 1  $\mu\text{m s}^{-1}$ . Thus, the contact time between the protein-modified tip and the substrate was less than 1 s. The same velocity was used for all measurements. A force–distance ( $f$ – $d$ ) curve was plotted by recording the forces acting between the surface and tip. As the monolayer surface approached the protein-immobilized AFM tip, the cantilever deflected due to attraction. The magnitude of the force was calculated by multiplying the spring constant of the cantilever (0.05 N m<sup>-1</sup>) by the cantilever's deflection distance. A further approach yielded a repulsive force between the substrate and tip. The repulsive force arising from the approach was 1 nN in all the measurements. After contact, the substrates were retracted from the tip. During the retraction, a “pull-off” force was observed, reflective of the detachment of the monolayer substrate from the protein-immobilized tip. The “adhesion force” was defined as the maximum pull-off force during retraction of the monolayer from the AFM tip.

### 2.3 Protein adsorption onto the OTS monolayers

Protein adsorption measurements were carried out in two steps. The freshly prepared OTS monolayers were immersed in the protein solution (1 mg mL<sup>-1</sup>, pH 7.4) at 28 °C. The immersion time was varied from 0 to 90 min. The samples were then immediately transferred into a 1 wt% sodium dodecyl sulfate (SDS) PBS aqueous solution and incubated for 1 h to detach the adsorbed proteins from the OTS monolayers. After desorption, the samples were immersed in deionized water for 30 s for rinsing, immediately followed by vacuum drying. A control experiment was conducted as follows. The substrates were immersed in the protein solution and then transferred to an

aqueous PBS solution without SDS for 1 h to allow desorption. The substrates were then immersed in deionized water for 30 s. The topologies of the residual protein layers remaining on each OTS-presenting silicon wafer after the completion of the experiments were examined by AFM (NanoscopeIII, Digital Instruments) operated in the tapping mode. The thickness of the protein layer deposited onto the OTS-monolayer over 90 min was measured by ellipsometry.

### 3 Results and discussion

#### 3.1 Characterizations of the octadecyltrichlorosilane (OTS) monolayers on silicon wafers

The conformations of the OTS chains on the silicon substrates were modulated by varying the preparation temperature. Briefly, an OTS–toluene solution was equilibrated in a reaction flask at either 5 °C or 50 °C under Ar flow, and a cleaned silicon wafer was placed into the flask. The reaction between the wafer and OTS proceeded over a maximum of 2 h to avoid the generation of a thick OTS film on the silicon wafer. After the reaction, the substrate was washed, baked, sonicated, and again washed to prepare the OTS monolayer. RA-FTIR analysis of the OTS monolayers prepared at 5 °C revealed symmetric and asymmetric stretching peaks corresponding to CH<sub>2</sub> groups at 2850 and 2919 cm<sup>-1</sup>, respectively. In contrast, the OTS monolayers prepared at 55 °C yielded peaks at 2854 and 2924 cm<sup>-1</sup> (Fig. 1). The shift toward higher wavenumbers in the monolayers prepared at higher temperatures implied a higher degree of intermolecular disorder in the monolayer.<sup>19–21</sup> Increasing the preparation temperature from 5 to 55 °C also reduced the thickness of the monolayer from 2.4 ± 0.1 nm to 1.5 ± 0.07 nm, as measured by ellipsometry. The melting temperature of the OTS monolayer was approximately 30 °C.<sup>19–21</sup> Therefore, OTS monolayers prepared at 50 °C were expected to have a higher degree of intermolecular disorder than those prepared at 5 °C because the OTS molecules were likely to collapse and pack in a lower density on the silicon substrate. Meanwhile, changes in the preparation temperature minimally affected the surface topology/roughness, as investigated by the AFM images (data not shown).<sup>19</sup> The results suggested that the OTS molecules at

both temperatures were uniformly tethered onto the silicon wafer without segregation or island formation. The uniformity was further confirmed by measuring the equilibrium water contact angles on these monolayers. For the OTS monolayers prepared at 5 °C and 55 °C, the contact angles were 107.0 ± 0.8° and 104.0 ± 1.1°, respectively, and there was no hysteresis. The slightly lower contact angle for the monolayers prepared at 50 °C probably resulted from CH<sub>2</sub> exposure in the less densely packed OTS monolayers.<sup>13a</sup>

#### 3.2 The adhesion strength of the proteins on the OTS monolayers

The adhesion strengths of the proteins on substrates with different degrees of disorder among the OTS chains were evaluated on the nano-Newton scale using AFM tips chemically functionalized with BSA or HF. Fig. 2 shows the *f*–*d* curves obtained between the AFM tips and OTS-monolayers. Over the course of recording 60–70 *f*–*d* curves using one AFM tip and one monolayer, no noticeable changes in the *f*–*d* curve shape were observed. This indicated that the proteins did not extensively detach from the AFM tips and the monolayer conformation did not change significantly during the measurements. A higher degree of intermolecular disorder (in the monolayer prepared from the solution at 50 °C) resulted in a higher protein adhesion

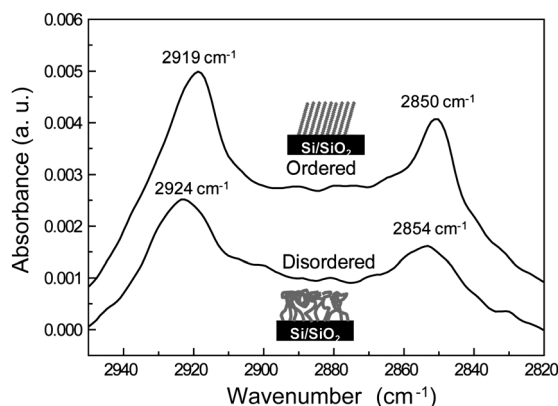


Fig. 1 RA-FTIR spectra of the ordered and disordered OTS monolayer surfaces.

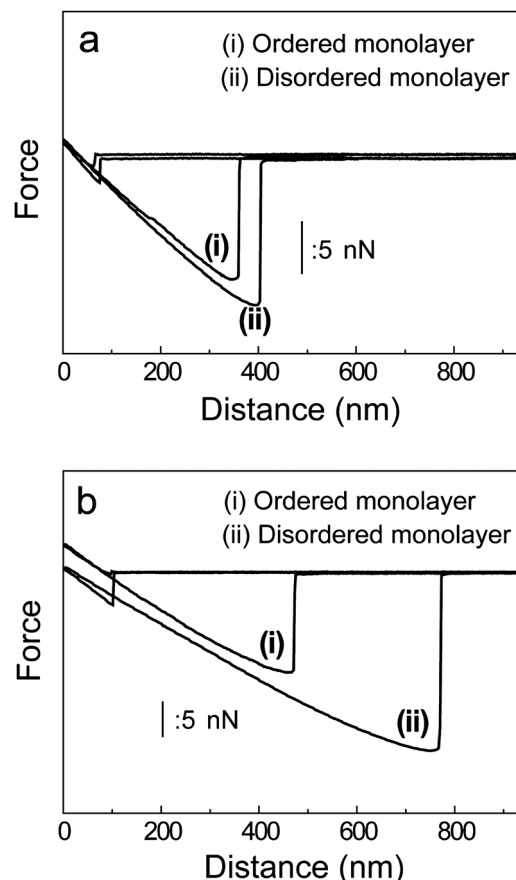


Fig. 2 Force–distance curves for the OTS monolayers and the protein-immobilized tips: (a) BSA and (b) HF.

strength (measured during the retraction of the OTS monolayer from the tip) for both BSA (Fig. 2a) and HF (Fig. 2b). Fig. 3 shows the histograms of the adhesion forces between the OTS monolayers and the tips. Each histogram was obtained by aggregating the data collected from 3 independent samples (using 3 sets of AFM tips and monolayers). The BSA-modified tips displayed adhesion forces in the presence of the ordered OTS monolayer of 6–20 nN, with the most common values in the range of 8–10 nN. The BSA-modified tip on the disordered OTS monolayer yielded an adhesion force of 10–20 nN, with the most common values in the range of 12–14 nN. The HF-modified tip in the presence of the ordered OTS monolayer displayed an adhesion force of 8–23 nN, with the most common values in the range of 8–12 nN. In the presence of the disordered OTS monolayer, the HF-modified tip displayed an adhesion force of 22–30 nN, with the most common values in the range of 25–26 nN. It is worth noting that the asymmetric histogram for the HF-modified tip in the presence of the ordered OTS monolayer (Fig. 3c) resulted from the aggregation of data from 3 independent tests: the result was not due to a trend (*e.g.*, an increase in the adhesion force over time) during the measurement. The statistical analysis showed that the dependence of the HF adhesion strength on the degree of disorder of the OTS molecules exceeded the corresponding dependence of BSA (Fig. 4).

The adhesion energies required during retraction were calculated by integrating the area under the *f*-*d* curve (Fig. 2). For BSA, the energy increased from  $2.45 \times 10^{-15}$  J to  $3.08 \times 10^{-15}$  J, and for HF, the energy increased from  $3.62 \times 10^{-15}$  J to  $9.7 \times 10^{-15}$  J, from the ordered to the disordered surface. The adhesion energy per protein was also estimated from the *f*-*d* curves (Fig. 2), the surface area of the AFM tip, and the molecular size of each protein (see the ESI†). For HF, the energies were estimated to be  $1.36 \times 10^{-16}$  and  $3.64 \times 10^{-16}$  J per HF molecule for the ordered and disordered OTS monolayers,

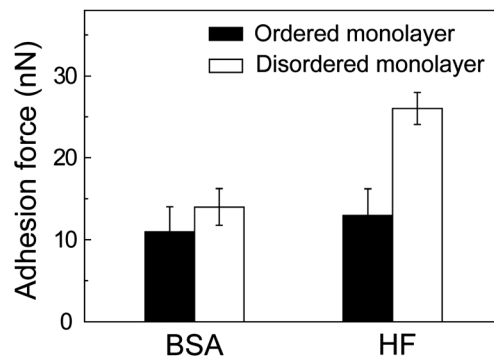


Fig. 4 The average adhesion force between the OTS monolayers and the protein-immobilized tips.

respectively. For BSA, the energies were  $1.99 \times 10^{-17}$  and  $2.51 \times 10^{-17}$  J per BSA molecule for the ordered and disordered OTS monolayers, respectively.

Interestingly in our results, the proteins showed different adhesion strengths depending on the conformations of the monolayers, even after short periods of contact (<1 s). Although the water contact angles of the two monolayers differed by  $3^\circ$ , this difference was not expected to significantly affect the protein adhesion strength. It was reported that less densely packed monolayers facilitate the penetration of protein molecules into a monolayer.<sup>13–15</sup> Combining our results and the previous reports, proteins may respond differently to monolayers with different conformations, thereby inducing different adhesion strengths. It is possible that the proteins and the disordered OTS molecules adhered by interlocking more strongly, and greater energy was required to separate the proteins from the disordered than from the ordered OTS monolayer (see Fig. 5).

It is worth noting that the adhesion energies of HF were higher than those of BSA in the presence of either monolayer. BSA molecules are globular in conformation,<sup>22</sup> whereas two of

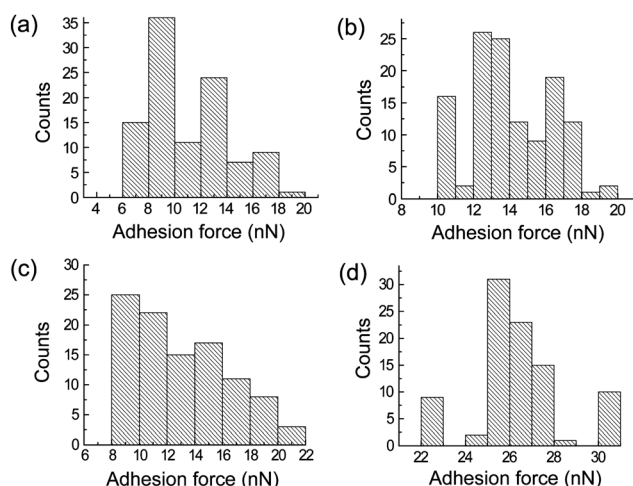


Fig. 3 Histograms of the maximum adhesion force (during retraction) between the OTS monolayers and the protein-immobilized tips: (a) between the ordered OTS monolayer and the BSA-immobilized tip; (b) between the disordered OTS monolayer and the BSA-immobilized tip; (c) between the ordered OTS monolayer and the HF-immobilized tip; and (d) between the disordered OTS monolayer and the HF-immobilized tip.

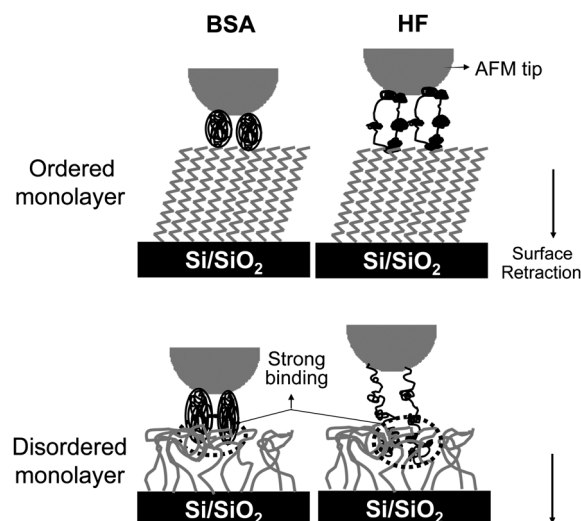
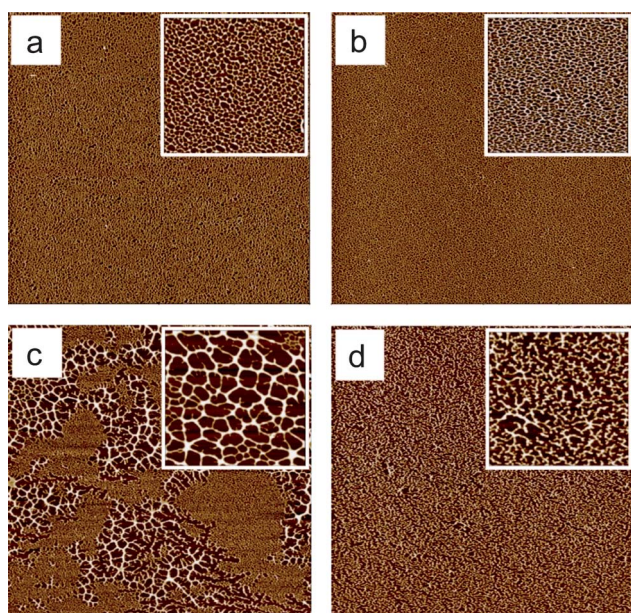


Fig. 5 Schematic diagrams illustrating adhesion between the protein-immobilized tips and the OTS monolayers.

the six domains of HF (D and  $\alpha$ C) are unstable.<sup>23,24</sup> As the HF molecules are quite flexible,<sup>25</sup> this flexibility may facilitate adhesive interactions with the OTS monolayers and increase the strength of the adhesive interactions relative to those of BSA. More importantly, from our results, the molecular structure of the proteins altered the degree of OTS monolayer's disordering effect on the adhesion strength with the proteins; however, the role of the chain flexibility in HF may be reduced in the presence of the ordered OTS monolayer due to the weak binding of the proteins to the ordered monolayer.

### 3.3 Adhesion of proteins onto the OTS monolayers based on the adsorption studies

The adhesion strengths of the proteins on the OTS monolayers were further evaluated by characterizing the topologies of the OTS monolayers after protein adsorption and subsequent washing with a wash solution. The experiment was designed to investigate the ability of the adsorbed proteins to resist detachment from the OTS monolayers after a long period of time (>30 s) in contact with the monolayers, which would predict the adhesion strength between the proteins and the substrates. The two OTS substrates were exposed to a protein PBS solution at 28 °C. An initial adsorption time of 90 min was used for both proteins. After adsorption, the substrates were immersed in a wash solution for 1 h. The wash solution contained sodium dodecyl sulfate (SDS) dissolved in an aqueous PBS solution. The protein coverage and adsorption patterns on the OTS monolayers were observed by AFM imaging. For comparison, we obtained control images of the substrates exposed to the protein solution and immersed in PBS (without SDS).



**Fig. 6** AFM images of BSA adsorbed onto the OTS monolayers after 90 min, followed by immersion in either (a and b) PBS aqueous solution or (c and d) SDS dissolved in an aqueous PBS solution for 1 h: (a and c) for the ordered OTS monolayer and (b and d) for the disordered OTS monolayer. The image areas correspond to  $10 \times 10 \mu\text{m}^2$  and the insets correspond to  $2 \times 2 \mu\text{m}^2$ .

**Table 1** Ellipsometric thicknesses of the protein layers adsorbed onto the OTS monolayers after washing either with PBS or a washing solution (SDS solubilized in PBS aqueous solution)

Proteins	Ordered monolayer		Disordered monolayer	
	PBS wash	Detergent wash	PBS wash	Detergent wash
BSA	$2.4 \pm 0.1$ nm	$0.8 \pm 0.4$ nm	$2.0 \pm 0.1$ nm	$1.9 \pm 0.3$ nm
HF	$5.4 \pm 0.2$ nm	$2.1 \pm 0.2$ nm	$5.3 \pm 0.1$ nm	$2.3 \pm 0.2$ nm

Fig. 6 shows AFM images of BSA adsorbed onto the OTS monolayers. For the control experiment (a and b), the two substrates displayed similar topologies after a protein adsorption incubation period of 90 min and a subsequent gentle rinse with PBS. In the meantime, the surface topologies of the two substrates covered with proteins differed significantly after washing the protein-adsorbed substrates with the wash solution (c and d). The BSA may have been more readily washed away from the ordered OTS monolayer than from the disordered monolayer. The average thickness of the protein layer on the disordered OTS monolayer, as measured by ellipsometry (see Table 1), was higher than the thickness of proteins on the ordered OTS monolayer.

Fig. 7 shows the surface topologies of the OTS monolayers after an HF adsorption incubation period of 90 min followed by rinsing with either PBS (a and b) or the wash solution (c and d). After washing with PBS, the surface topologies of the two substrates were found to be essentially identical: the surfaces were very smooth and without defects. Although washing with the wash solution removed some of the proteins from the

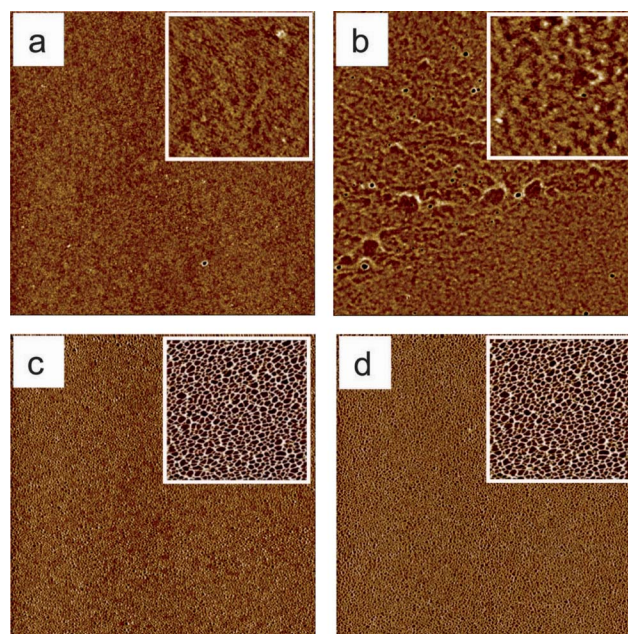


**Fig. 7** AFM images of the HF layer adsorbed onto the OTS monolayers after 90 min, followed by immersion in either (a and b) PBS aqueous solution or (c and d) SDS dissolved in an aqueous PBS solution for 1 h: (a and c) for the ordered OTS monolayer and (b and d) for the disordered OTS monolayer. The image areas correspond to  $10 \times 10 \mu\text{m}^2$  and the insets correspond to  $2 \times 2 \mu\text{m}^2$ .

substrates, the topologies of the two substrates did not differ significantly. In addition, the average thicknesses of the protein layers on either monolayer were essentially identical under the two conditions.

Fig. 6 and 7 may suggest that HF adhered to the substrates more strongly than BSA. These results were consistent with the results of the adhesion force measurements. However, HF molecules adhered to both monolayers with similar adhesion strengths after a protein adsorption incubation period of 90 min, while BSA displayed different adhesion strengths over the same timescale. In contrast with the results from BSA, the HF molecules appeared to adhere strongly to both substrates over a 90 min protein adsorption time. To clarify the similar adhesion of HF for both monolayers at this adsorption time, we conducted a series of HF adsorption experiments over several adsorption times. In all experiments, the SDS PBS aqueous solution was used for washing, and the washing time was held constant at 1 h. Fig. 8 shows the adsorption time-dependent topologies of the ordered OTS monolayer substrates. The HF molecular coverage was initially very low (Fig. 8a and b), but the coverage gradually increased with the adsorption time. In

addition, different topologies were observed at early adsorption time (0–120 s). It was worth noting that the images shown in Fig. 8a–c did not arise from the debris introduced during imaging or defects in the monolayer. The nodes in the images were similar to those reported previously for adsorbed HF.<sup>26</sup> Beyond an incubation time of 180 s (Fig. 8e), the ordered OTS monolayer surface was uniformly covered with the HF molecules. In contrast, the HF molecules covered the disordered OTS monolayer more rapidly than the ordered OTS monolayer (Fig. 9), and more proteins were present on the disordered substrate than on the ordered substrate after an adsorption time of 30 or 60 s. Although the disordered OTS monolayer displayed different topologies at 90 s with HF, the two topologies were not much different as in the case of ordered OTS monolayers (0–120 s).

These results suggested that the adhesion strengths of the proteins and the resistance of the proteins to detachment were higher for the disordered monolayer than for the ordered monolayer. The adsorption studies additionally showed that different adsorption times were required for the two proteins to

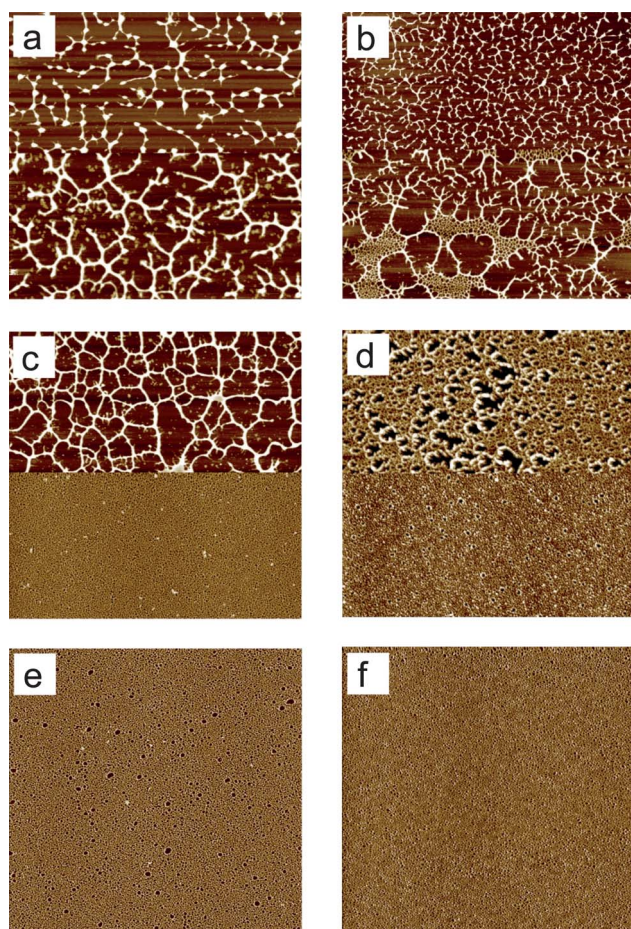


**Fig. 8** AFM images of HF adsorbed onto the ordered OTS monolayers as a function of the adsorption time. After adsorption, the samples were immersed in detergent for 1 h. The adsorption times for each sample were (a) 30 s; (b) 60 s; (c) 90 s; (d) 120 s; (e) 180 s and (f) 90 min. (a)–(d) show the two distinct topologies. The image areas correspond to  $10 \times 10 \mu\text{m}^2$ .

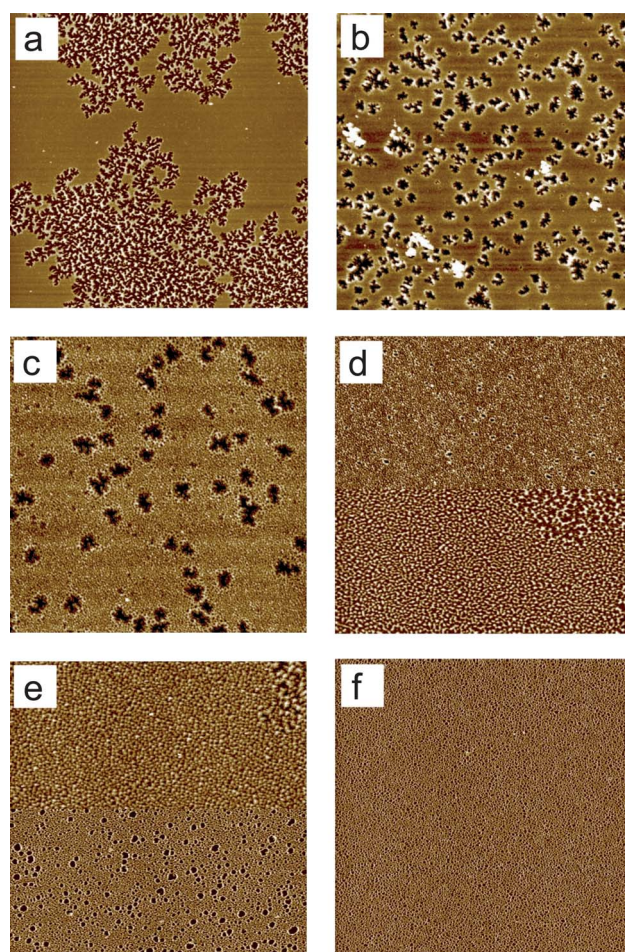


**Fig. 9** AFM images of HF adsorbed onto the disordered OTS monolayers as a function of the adsorption time. After adsorption, the samples were immersed in detergent for 1 h. The adsorption times for each sample were (a) 30 s; (b) 60 s; (c) 90 s; (d) 120 s; (e) 180 s and (f) 90 min. (d) shows the two distinct topologies. The image areas correspond to  $10 \times 10 \mu\text{m}^2$ .

achieve different levels of adhesion to the substrates. The adhesion strength of BSA on the ordered OTS substrate remained weak compared to the adhesion strength on the disordered substrate, even after a 90 min adsorption time. On the other hand, differences in the adhesion strength were observed for HF only on short adsorption timescales of less than 1 min. After 90 s, HF did not display any differences in the adhesion strength. These results indicated that the HF molecules adhered to the OTS monolayers strongly and rapidly, regardless of the OTS conformation, even when HF remained only for a few minutes.

To investigate any difference in adsorption patterns of HF for the two monolayers over the adsorption period, sectional analysis of the AFM images was conducted, yielding interesting results for the ordered OTS monolayers (Fig. 10a). The heights of the HF molecules attached to the ordered substrates were fairly large, 25–40 nm after 30 s. The height decreased with increasing adsorption time, reaching 6–7 nm. In contrast, the heights of the HF molecules adhered to the disordered substrate were lower than the heights on the ordered OTS for short adsorption times (Fig. 10b). Fig. 11 shows plots of the average heights of the HF molecules on the two OTS monolayers as a function of the adsorption time. The average height of the layer adsorbed onto the ordered OTS monolayer changed significantly from 33 nm at 30 s to 6 nm at 180 s, whereas the heights of the HF molecules on the disordered OTS layer were nearly constant for all adsorption times.

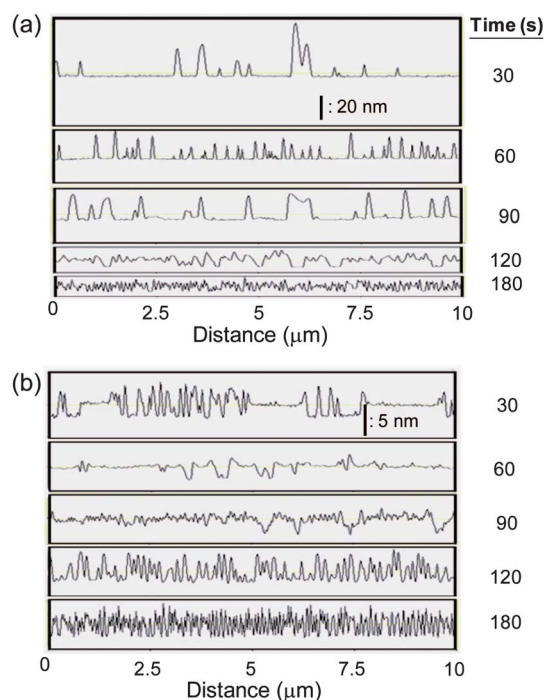


**Fig. 10** Sectional analysis of the AFM images of HF adsorbed onto the ordered OTS monolayers, as a function of the adsorption time. After adsorption, the samples were immersed in the washing solution for 1 h. (a) Ordered OTS monolayers and (b) the disordered OTS monolayers. The adsorption times are noted in the figures.

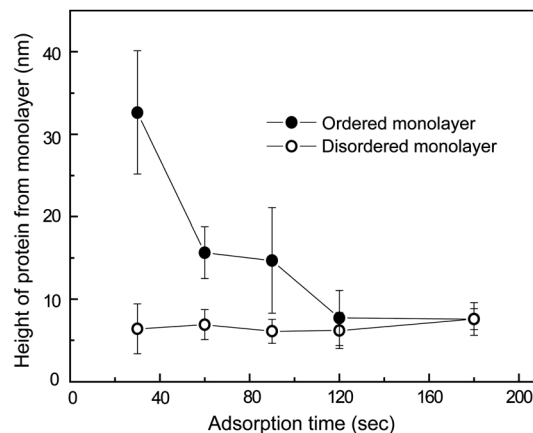


**Fig. 11** Average heights of the layer of HF molecules adsorbed onto the surfaces of the OTS monolayers, as a function of the adsorption time.

The reason underlying such results remains unclear. Several possibilities may be considered. The average protein layer height of 33 nm after a 30 s adhesion time was comparable to the longitudinal distance of the HF molecules (47 nm). The protein layer height of 6 nm, observed after 90 min adsorption, was comparable to the proposed width of HF (5 nm)<sup>23</sup> or slightly larger than the experimentally measured height for a single HF molecule.<sup>24,26</sup> These results might suggest that changes in the adsorption mode of HF, from end-on to side-on, may have altered the thickness of the protein layer;<sup>27</sup> however, there is a lack of evidence to support the notion that the height of the HF protein layer after 30 s adsorption time was solely due to an end-on height adsorption conformation in single molecules. Single molecule imaging revealed the heights of the HF molecules adsorbed onto a substrate, which were less than 2 nm and probably indicated side-on adsorption.<sup>26</sup> Therefore, at short periods of adsorption time, the extremely large heights of the HF molecules adsorbed onto the ordered OTS monolayer were attributable to lateral stacking among the proteins on top of proteins that were strongly adhered onto the substrates. During the early stages of adsorption onto the ordered OTS monolayer, HF molecules adsorbed randomly and filled the vacant sites (end-on adsorption) on the monolayer surface. Over time, the unstable protein molecules that had adsorbed during the initial stages of adsorption were displaced by stably anchored proteins.<sup>27</sup> In addition, the weakly bound proteins were removed during the washing step. In such a case, the different topologies on the ordered OTS monolayer at early adsorption times (Fig. 8a–c) might be due to the unstable adsorption. The fits to heights of HF for the ordered OTS monolayer, shown in Fig. 11, were used to estimate a characteristic time of 54 s from which the height of adsorbed HF was not significantly changed. From the AFM studies, it was also found that the adhesion force between HF and the ordered monolayers was increased to  $19 \text{ nN} \pm 1.5 \text{ nN}$  for the velocity of  $0.2 \mu\text{m s}^{-1}$  (for the velocity of  $1 \mu\text{m s}^{-1}$ , the ordered and disordered monolayers yielded  $13 \pm 3.2$  and  $26 \pm 2.0 \text{ nN}$ , respectively, as shown in Fig. 4). The results are probably implying that the HF molecules required some time to strongly adhere to the ordered OTS monolayer.

Meanwhile, the heights of the HF layers adhering to the disordered OTS substrate remained small for all adsorption times, suggesting that the HF molecules adhered to the disordered OTS monolayers strongly, even for short adsorption times.

## 4 Conclusion

This study examined the role played by the degree of molecular disorder in surface-modifying hydrocarbon chains in the regulation of protein adhesion behavior. Adhesion and adsorption studies showed that different adhesion behaviors were observed for BSA or HF in the presence of OTS monolayers having different degrees of molecular order. In addition, different timescales were observed for the different adhesion behaviors; HF displayed different adhesion behaviors on the two monolayers within very short adsorption periods or contact time (<1 min) whereas the BSA adhesion differed even for long adsorption times. The results of this study demonstrate the importance of the monolayer structure for regulating protein adhesion and adsorption behaviors. These results will be useful in applications involving cell adhesion regulation, array design, and proliferation, as well as in regulating protein patterns on substrates.

## Acknowledgements

This work was supported by a grant from the Center for Advanced Soft Electronics under the Global Frontier Research Program of the Ministry of Education, Science and Technology, Korea. E. C. Cho also acknowledges for the support by the Manpower Development Program for Energy (MKE).

## References

- (a) G. B. Sigal, M. Mrksich and G. M. Whitesides, *J. Am. Chem. Soc.*, 1998, **120**, 3464–3473; (b) K. L. Prime and G. M. Whitesides, *Science*, 1991, **252**, 1164.
- H. Elwing, S. Welin, A. Askendahl and I. Lunstrom, *J. Colloid Interface Sci.*, 1988, **123**, 306.
- J. L. Brash and T. A. Horbett, in *Proteins at Interfaces II*, ed. T. A. Horbett and J. L. Brash, American Chemical Society, Washington DC, 1995, p. 1.
- J. R. Capadona, D. M. Collard and A. J. Garcia, *Langmuir*, 2003, **19**, 1847.
- (a) S. Kidoaki and T. Matuda, *Langmuir*, 1999, **15**, 7639; (b) A. Sethuraman, M. Han, R. S. Kane and G. Belfort, *Langmuir*, 2004, **20**, 7779.
- (a) V. Slin, H. Weetall and D. J. Vanderah, *J. Colloid Interface Sci.*, 1997, **185**, 94; (b) P. S. Sit and R. E. Marchant, *Thromb. Haemostasis*, 1999, **82**, 1053; (c) S. Welin-Klinstrom, R. Jansson and H. Elwing, *J. Colloid Interface Sci.*, 1993, **157**, 498.
- M. Lestelius, B. Liedberg and P. Tengvall, *Langmuir*, 1997, **13**, 5900.
- W. Norde and J. Lyklema, *J. Colloid Interface Sci.*, 1978, **66**(498), 257.
- X. Chen, N. Patel, M. C. Davis, C. J. Roberts, S. J. B. Tendler, P. M. Williams, J. Davies, A. C. Dawkes and J. C. Edwards, *Appl. Phys. A: Mater. Sci. Process.*, 1998, **66**, S631.
- C. F. Wertz and M. M. Santore, *Langmuir*, 2001, **17**, 3006.
- P. Roach, D. Farrar and C. C. Perry, *J. Am. Chem. Soc.*, 2006, **128**, 3939.
- L. Li, S. Chen and S. Jiang, *Langmuir*, 2003, **19**, 2974.
- (a) S. Petrash, N. B. Sheller, W. Dando and M. Foster, *Langmuir*, 1997, **13**, 1881; (b) E. J. Choi and M. D. Foster, *Langmuir*, 2002, **18**, 557.
- N. B. Sheller, S. Petrash and M. D. Foster, *Langmuir*, 1998, **14**, 4535.
- S. Petrash, T. Cregger, B. Zhao, E. Pokidysheva, M. D. Foster, W. J. Brittan, V. Sevastianov and C. F. Majkrzak, *Langmuir*, 2001, **17**, 7645.
- (a) M. Mrksich, *Chem. Soc. Rev.*, 2000, **29**, 267; (b) B. Kasemo, *Curr. Opin. Solid State Mater. Sci.*, 1998, **3**, 451; (c) S. P. Paleck, J. C. Loftus, M. H. Ginsberg, D. A. Lauffenburger and A. F. Horwitz, *Nature*, 1997, **385**, 537; (d) A. J. Garcia, M. D. Vega and D. Boettiger, *Mol. Biol. Cell*, 1999, **10**, 785; (e) Y. Tamada and Y. Ikada, *J. Colloid Interface Sci.*, 1993, **155**, 334.
- C. F. Wertz and M. M. Santore, *Langmuir*, 1999, **15**, 8884.
- (a) H. J. Kong, J. Liu, K. Riddles, T. Matsumoto, K. Leach and D. J. Mooney, *Nat. Mater.*, 2005, **4**, 460; (b) H. J. Kong, S. Hsiong and D. J. Mooney, *Nano Lett.*, 2007, **7**, 161; (c) N. Singh, X. Cui, T. Boland and S. M. Husson, *Biomaterials*, 2007, **28**, 763; (d) M. Veiseh, M. H. Zareie and M. Zhang, *Langmuir*, 2002, **18**, 6671.
- (a) D. Lee, D. Kim, T. Oh and K. Cho, *Langmuir*, 2004, **20**, 8124; (b) D. Lee, T. Oh and K. Cho, *J. Phys. Chem. B*, 2005, **109**, 11301.
- (a) K. Imura, Y. Nakajima and T. Kato, *Thin Solid Films*, 2000, **379**, 230; (b) R. R. Rye, *Langmuir*, 1997, **13**, 2588.
- J. B. Brzoska, I. B. Azouz and F. Rondelez, *Langmuir*, 1994, **10**, 4367.
- D. C. Carter and X. M. He, *Science*, 1990, **249**, 302; X. M. He and D. C. Carter, *Nature*, 1992, **358**, 209.
- J. W. Weisel, C. V. Stauffacher, E. Bullitt and C. Cohen, *Science*, 1985, **230**, 1388.
- A. Toscano and M. M. Santore, *Langmuir*, 2006, **22**, 2588.
- L. Feng and J. D. Andrade, in *Proteins at Interfaces II*, ed. T. A. Horbett and J. L. Brash, American Chemical Society, Washington DC, 1995, p. 66.
- K. L. Marchin and C. L. Berrie, *Langmuir*, 2003, **19**, 9883.
- J. D. Andrade, in *Surface and Interfacial Aspects of Biomedical Polymers. Protein Adsorption*, ed. J. D. Andrade, Plenum Press, New York, 1985, p. 1.